



Polymer Nanofiber-Embedded Microchips for Detection, Isolation, and Molecular Analysis of Single Circulating Melanoma Cells**

Shuang Hou, Libo Zhao, Qinglin Shen, Juehua Yu, Charles Ng, Xiangju Kong, Dongxia Wu, Min Song, Xiaohong Shi, Xiaochun Xu, Wei-Han OuYang, Rongxian He, Xing-Zhong Zhao, Tom Lee, F. Charles Brunicardi, Mitch André Garcia,* Antoni Ribas,* Roger S. Lo,* and Hsian-Rong Tseng*

Circulating tumor cells (CTCs)^[1] are cancer cells shed from either primary tumors or metastatic sites. The presence and number of CTCs in peripheral blood can provide clinically important data on prognosis and therapeutic response patterns, respectively.^[2] Thus, as with traditional invasive tumor biopsies that enable gold-standard pathological analysis, CTCs can be regarded as “liquid biopsies” of the tumor, which enable repeated and relatively non-invasive characterization of tumor evolution, especially important during therapeutic interventions. Currently, the FDA-approved CellSearch assay is costly and inefficient at capturing CTCs, and the enriched CTCs are typically contaminated with a large number of white blood cells (WBCs). As a result, the diagnostic value of CTCs has been underused. Over the past decade, a diversity of CTC detection methods^[2d,3] have been developed to overcome the challenges encountered by the immunomagnetic-separation-based CellSearch assay.

Different from the existing CTC diagnostic approaches,^[2d,3] we have demonstrated “nanovelcro” chips^[4] that are capable of enriching, identifying, and enumerating CTCs in patient blood samples with superb efficiency. First, we pioneered a unique concept of nanovelcro substrates,^[5] by which anti-EpCAM-coated silicon-nanowire (SiNW) substrates were used to immobilize CTCs in a stationary device. We have recently shown that other types of nanostructured substrates (e.g., electrochemically deposited con-

jugated-polymer nanofeatures^[6] and horizontally packed TiO₂ nanofibers^[7]) also exhibit enhanced affinity for capturing CTCs, demonstrating the general applicability of nanovelcro substrates. Our approach is unique because of the use of nanostructured substrates; there are enhanced local topographic interactions^[8] between the anti-EpCAM-coated nanosubstrates and the nanoscaled cellular surface components (e.g., microvilli) on a CTC, which are analogous to the working principle of velcro. Second, by integrating a lithographically patterned nanovelcro substrate with an overlaid poly(dimethylsiloxane) (PDMS) chaotic mixer^[9] that enhances the frequency of contact between the CTCs flowing through the system and the substrate, we further improved CTC capture efficiency.^[4] Side-by-side analytical validation studies using both artificial and patient CTC samples suggested that the sensitivity of nanovelcro chips outperformed^[4] that of CellSearch. Although nanovelcro chips allow efficient and reproducible detection of CTCs in patient blood, challenges remain in 1) broadening its general applicability for detecting other types of solid-tumor CTCs that exhibit surface markers other than EpCAM, and 2) enabling the isolation of single CTCs for subsequent molecular analyses. To broaden the general applicability of the nanovelcro-based cell-affinity assay, we explored a melanoma-specific capture agent^[13] (i.e., anti-CD146) to capture circulating melanoma cells (CMCs; a subcategory of solid-tumor CTCs). Further, an

[*] Dr. S. Hou,^[†] Dr. L. Zhao,^[†] Q. Shen,^[†] Dr. D. Wu, Dr. M. Song,

Dr. X. Shi, T. Lee, Prof. H.-R. Tseng
Department of Molecular and Medical Pharmacology
Crump Institute for Molecular Imaging (CIMI)
California NanoSystems Institute (CNSI)
University of California, Los Angeles
570 Westwood Plaza, Building 114
Los Angeles, CA 90095-1770 (USA)
E-mail: hrttseng@mednet.ucla.edu
Homepage: <http://www.tseng-lab.com>

X. Kong, Prof. R. S. Lo
Division of Dermatology, Department of Medicine
University of California, Los Angeles
E-mail: rlo@mednet.ucla.edu
C. Ng, Prof. A. Ribas
Division of Hematology and Oncology, Department of Medicine
Department of Surgery, and
Department of Molecular and Medical Pharmacology
University of California, Los Angeles (USA)
E-mail: aribas@mednet.ucla.edu

Dr. J. Yu,^[†] Prof. F. C. Brunicardi
Department of Surgery
University of California, Los Angeles (USA)

X. Xu, W.-H. OuYang, Dr. M. A. Garcia
CytoLumina Technologies Corp.
21038 Commerce Point Dr., Walnut, CA 91789 (USA)
E-mail: mgarcia@cytolumina.com

Q. Shen,^[†] R. He, Prof. X.-Z. Zhao
Department of Applied Physics and Department of Oncology
Surgery, Wuhan University
Wuhan (P.R. China)

[†] These authors contributed equally to the work.

[**] This research was supported by the National Institutes of Health (R21 CA151159 and R33 CA157396). Dr. F. Charles Brunicardi, Dr. Antoni Ribas, Dr. Roger S. Lo, and Dr. Hsian-Rong Tseng are members of UCLA Josson Comprehensive Cancer Center. They acknowledge generous support from JCCC and promotion of the collaboration.



Supporting information for this article is available on the WWW under <http://dx.doi.org/10.1002/anie.201208452>.

increasing number of studies have shown extensive molecular heterogeneity^[10] in CTCs from the same types of cancer or even the same patient.^[11] Therefore, it is important to develop single-CTC isolation methods that enable single-cell molecular analyses to better understand the origin and role(s) of CTCs in cancer progression.

To improve on our previously reported nanovelcro chips,^[4] we introduced the next-generation of nanovelcro chip (i.e., poly(lactic-co-glycolic acid) (PLGA)-nanofiber-embedded nanovelcro chip, abbreviated PN-nanovelcro chip; Figure 1 a,b) capable of not only capturing CMCs with high

to specifically identify CMCs among nonspecifically captured WBCs. After CMC capture and ICC melanoma lineage validation, an LMD microscope was used to cut out and harvest single CMCs for subsequent Sanger sequence analysis. To examine the clinical utility of the optimized PN-nanovelcro chips, we then performed single-CMC isolation and genotyping using peripheral blood samples collected from two stage-IV melanoma patients, whose melanomas have been previously characterized by conventional PCR-based techniques (cobas 4800, Roche) to contain a signature oncogenic mutation (i.e., *BRAF*^{V600E}). Over the past few

years, there has been a drastic change in the treatment of metastatic melanoma. BRAF inhibitors (e.g., vemurafenib) designed to target melanomas that are driven by the *BRAF*^{V600E} mutation have shown unprecedented success, eliciting responses in more than 80 % of patients and conferring survival benefits.^[15] Thus, the test for the *BRAF*^{V600E} mutation (which is present in 60 % of melanomas), developed as a companion diagnostic to the clinical development of the BRAF inhibitor vemurafenib, provides an indispensable biomarker prior to initiating BRAF inhibitor therapy among melanoma patients.

The PN-nanovelcro chip is composed of two functional components (Figure 1 a,b), including an overlaid PDMS chaotic mixer^[4] (Figure 1 e) and a transparent PN-nanovelcro substrate, which were assembled in a plastic chip holder (using four parallel-oriented screws). A 22 cm-long microchannel with embedded herringbone features^[9] for increasing cell-substrate contact frequency was fabricated into the PDMS chaotic mixer (Figure 1 e). A custom-designed electrospinning system^[7] (see Supporting Information) was employed to deposit PLGA nanofibers (130.6 ± 62.7 nm in diameter, Figure 1 c; also see Supporting Information) onto an LMD slide (Leica; with a pre-deposited 1.2 μm -thick poly(phenylene sulfide), PPS membrane) to generate transparent PN-nanovelcro substrates. *N*-hydroxysuccinimide (NHS) chemistry was used to activate the carboxylic acid groups on the surface of the PLGA nanofibers for covalent conjugation of streptavidin (Figure 1 d). A syringe pump and syringes were used to introduce

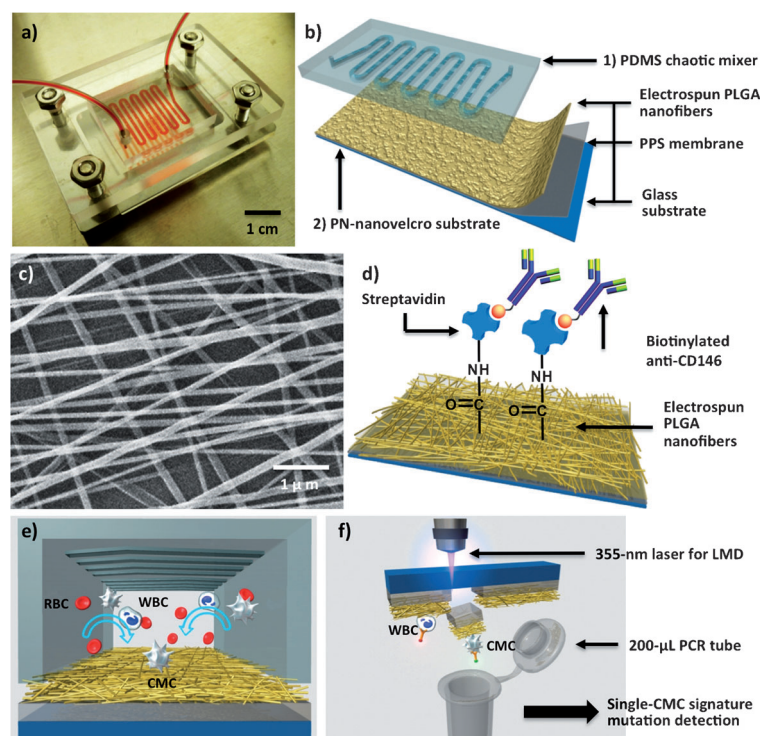


Figure 1. a) Photograph of a PN-nanovelcro chip for capture and isolation of single CMCs. b) A PN-nanovelcro chip is composed of 1) an overlaid PDMS chaotic mixer and 2) a transparent PN-nanovelcro substrate. c) SEM image of electrospun PLGA nanofibers on a PN-nanovelcro substrate. d) NHS chemistry is used to covalently anchor streptavidin for conjugation of biotinylated anti-CD146, a melanoma-specific antibody. e) Scheme of the mechanism of the PN-nanovelcro CMC chip. f) Method of LMD-based single-CMC isolation.

efficiency, but also enabling highly specific isolation of single CMCs immobilized on the nanosubstrate without contamination by WBCs. The goal was to replace the non-transparent SiNW substrate in the earlier nanovelcro chip^[4] with a transparent PN-nanovelcro substrate, prepared by depositing electrospun PLGA nanofibers^[12] (Figure 1 c) onto a commercial laser microdissection (LMD) slide, followed by streptavidin-mediated conjugation of a melanoma-specific antibody^[13] (i.e., anti-CD146, Figure 1 d). The unique combination of PLGA nanofibers and an LMD slide enables single CMC isolation using a highly accurate LMD technique. We first used melanoma cell lines to optimize and validate the performance of the PN-nanovelcro chips. In parallel, a four-color immunocytochemistry (ICC) method^[14] was established

cell suspensions or blood samples, ethanol for fixation and permeabilization, and ICC agents into the PN-nanovelcro chips with controlled flow rates. Prior to the cell-capture studies, biotinylated anti-CD146 ($8 \mu\text{g mL}^{-1}$ in $500 \mu\text{L}$ PBS with 1 % (w/v) BSA) was freshly grafted onto the PN-nanovelcro substrates.

To optimize and validate the performance of PN-nanovelcro chips, we prepared suspensions of the M229 human melanoma cell line^[16] ($100 \text{ cells mL}^{-1}$ in DMEM medium) as a model system. We first examined how different electrospinning times affected the CMC capture efficiency. Using a flow rate of 1.0 mL h^{-1} ,^[3e,4,9] the optimal deposition time of three hours (Figure 2 a, corresponding to a $3 \mu\text{m}$ -thick PLGA-nanofiber membrane, confirmed by profilometer) led to

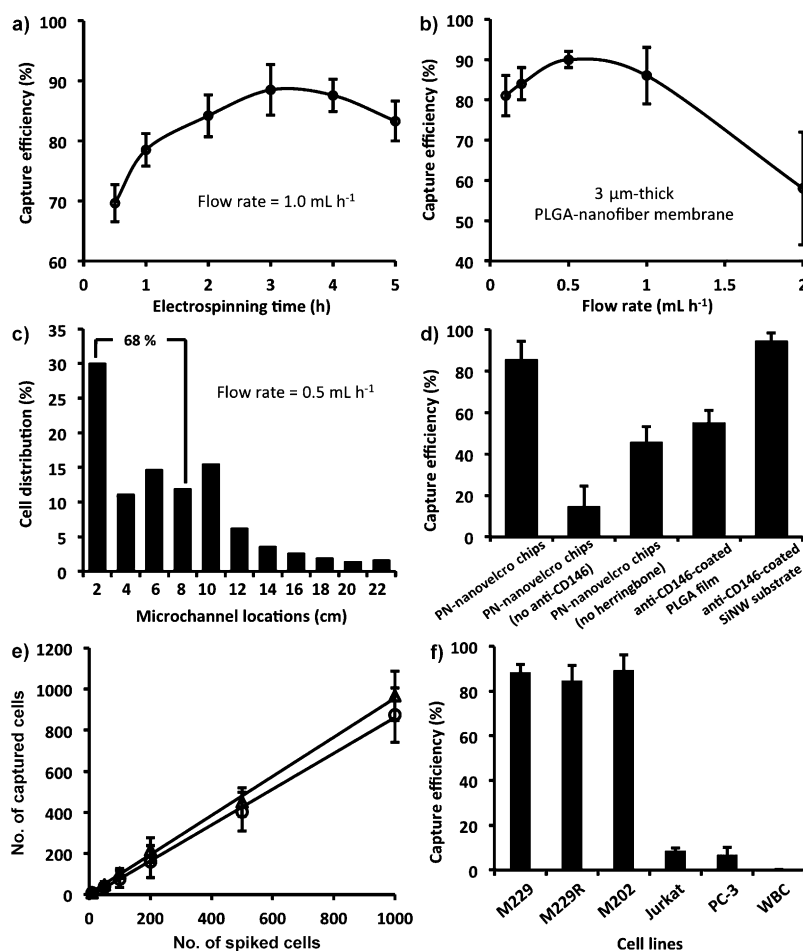


Figure 2. Optimization and validation of PN-nanovelcro chips using M229 melanoma cells (error bars show standard deviations, $n \geq 3$). a) Capture efficiency obtained as the function of electrospinning deposition time. b) Based on the optimal electrospinning time of 3 h, capture efficiencies were measured at different flow rates. c) Spatial distribution of substrate-immobilized cells along the microchannel. d) Comparison of cell capture efficiency between anti-CD146-coated PN-nanovelcro chips and four different control systems. e) Capture efficiency at different cell numbers in both DMEM medium (Δ) and whole blood (\circ). f) Capture efficiency using suspensions of melanoma cells (M229, M229R, and M202), T-lymphocyte (Jurkat), prostate (PC3), and WBCs.

approximately 87% capture efficiency. By applying 3 μm -thick PLGA-nanofiber membranes in the devices, we then found that a slower flow rate of 0.5 mL h^{-1} (Figure 2b) improved the capture of cells. We analyzed the spatial distribution (Figure 2c) of substrate-immobilized cells at different locations along the 22 cm microchannel. At a flow rate of 0.5 mL h^{-1} , 68% of the cells were captured in the first 8 cm of the microchannel, suggesting that the channel is sufficiently long to capture the cells. Further, four control studies using 1) PN-nanovelcro chips without anti-CD146, 2) PN-nanovelcro chips without herringbone microfeatures,^[9] 3) anti-CD146-coated PLGA films (3 μm thick, no nano-features), and 4) anti-CD146-coated SiNW substrates^[4] were carried out in parallel with CD146-coated PN-nanovelcro chips. The results of these controls suggest that the capture agent, microfluidic chaotic mixer,^[9] and nanostructures all play important roles in the superb cell capture observed

(Figure 2d). We also tested the dynamic range of the PN-nanovelcro chips using a series of artificial CMC samples that were prepared by spiking DMEM medium and healthy blood samples with DiO-stained M229 cells at densities of 10, 50, 100, 200, 500, and 1000 cells mL^{-1} . The results (Figure 2e) show that the devices exhibit sufficient performance for clinical samples, which usually have a CMC density of a few to hundreds of cells per milliliter. Finally, we tested the general applicability and specificity of PN-nanovelcro chips for capturing CD146-positive melanoma cells. Three CD146-positive melanoma cell lines^[16] (M229, M229R—a vemurafenib-resistant sub-line derived from M229, and M202) were studied in parallel with two CD146-negative cancer cell lines (Jurkat leukemia and PC3 prostate cancer cells) and freshly isolated human WBCs. PN-nanovelcro chips were capable of specifically capturing melanoma cells (Figure 2f), and non-specific immobilization of other types of cells could be mitigated using the subsequent ICC method and fluorescence LMD technique.

To examine the clinical utility of the PN-nanovelcro chips, we performed single-CMC isolation and genotyping on blood samples collected from two stage-IV melanoma patients whose metastatic tumors were confirmed to have the *BRAF*^{V600E} mutation. For comparison, an artificial sample was prepared by spiking 50 M229 cells (known to have a *BRAF*^{V600E} mutation) into 1.0 mL of blood from a healthy donor. After flowing blood samples through PN-nanovelcro chips, a four-color ICC method for parallel staining of FITC-labeled anti-Mart1, TRITC-labeled anti-HMW-MAA, DAPI, and Cy5-labeled anti-CD45 was established to identify CMCs (DAPI + /Mart1 + /HMW-MAA + /CD45 – and 40 μm > diameter > 10 μm) among non-specifically captured WBCs (DAPI + /Mart1 – /HMW-MAA – /CD45 + and diameter < 10 μm) and cellular debris, immobilized on PN-nanovelcro substrates. After performing ICC, the overlaid microfluidic chaotic mixer was removed, and the transparent PN-nanovelcro substrate with immobilized CMCs were mounted onto a fluorescent microscope (Nikon Ni) for identification, registration, and enumeration of CMCs (see Supporting Information for experimental details). 45, 43, and 36 CMCs were captured and identified from the 1.0 mL artificial control sample, patient 1, and patient 2 blood samples, respectively. Subsequently, a fluorescent microscope (Leica LMD7000) equipped with a 355 nm LMD setup was used to cut the PLGA nanofibers along with the supporting PPS membrane located underneath the pre-identified CMCs (Figure 3b), allowing the collection of a single CMC into a 200 μL PCR tube for whole-genome amplification and sequence analysis. Among the 45, 43, and 36 captured CMCs,

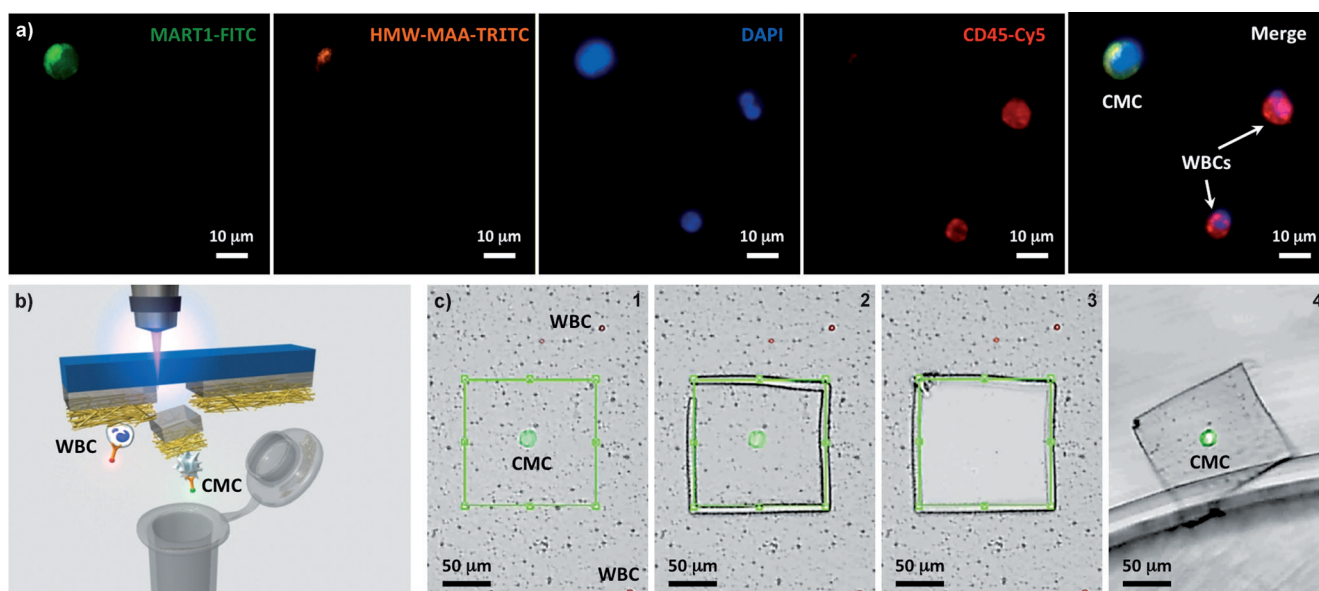


Figure 3. a) Typical micrographs of a CMC and WBCs immobilized on a PN-nanovelcro chip. A four-color ICC method for parallel staining with FITC-labeled anti-Mart1, TRITC-labeled anti-HMW-MAA, DAPI, and Cy5-labeled anti-CD45 was used to identify substrate-immobilized CMCs (DAPI + /Mart1 + /HMW-MAA + /CD45 – and 40 μm > diameter > 10 μm) from nonspecifically captured WBCs (DAPI + /Mart1 – /HMW-MAA – /CD45 + and diameter < 10 μm) and cellular debris. b) Method of LMD-based single-CMC isolation. c) Micrograph images of the LMD-based single CMC isolation: 1) identification of a CMC, 2) laser-dissection of the CMC, 3, 4) releasing the CMC from the substrate, followed by harvesting into a 200 μL PCR tube.

30, 24, and 18 CMCs were isolated by LMD for individual analyses.

A commercial whole-genome amplification kit^[11] (WGA kit, Sigma/Aldrich) was used to amplify genomic DNA (gDNA) from each CMC, and the resulting gDNA was then subjected to specific PCR amplification in the presence of BRAF exon 15 (containing the *BRAF*^{V600E} codon)-specific primers.^[16b] The double-amplified gDNA was then subjected to Sanger sequencing (Figure 4). We were able to detect the *BRAF*^{V600E} mutation from the M229-based control sample and CMCs isolated from both patient 1 and patient 2 blood samples. The *BRAF*^{V600E} mutation identified in the CMCs was consistent with those found in their tumor biopsies. As a negative control, WBCs isolated from the two melanoma patients showed no *BRAF*^{V600E} mutation. Notably, the Sanger sequencing data obtained for the *BRAF*^{V600E} mutation in single CMCs (Figure 4) displayed a strong signal-to-noise ratio. In contrast, varying levels of sequencing noise and *BRAF*^{V600E} zygosity are often encountered when traditional melanoma biopsies are sequenced, as a result of the standard tissue fixation method and tissue heterogeneity (“contamination” with stromal and immune cell types).^[17]

In conclusion, the continuing development of a nanovelcro CTC assay, including the replacement of the original non-transparent SiNW nanovelcro substrate with a new transparent PN-nanovelcro substrate to enable laser-assisted microdissection, has allowed for single-tumor-cell isolation, in addition to outstanding CMC capture. Furthermore, we were able to extend the applicability of this new PN-nanovelcro chip beyond epithelial cancers to specifically detect and isolate CMCs. Our proof-of-concept study validated this assay for CMC detection, isolation, and single-CMC genotyp-

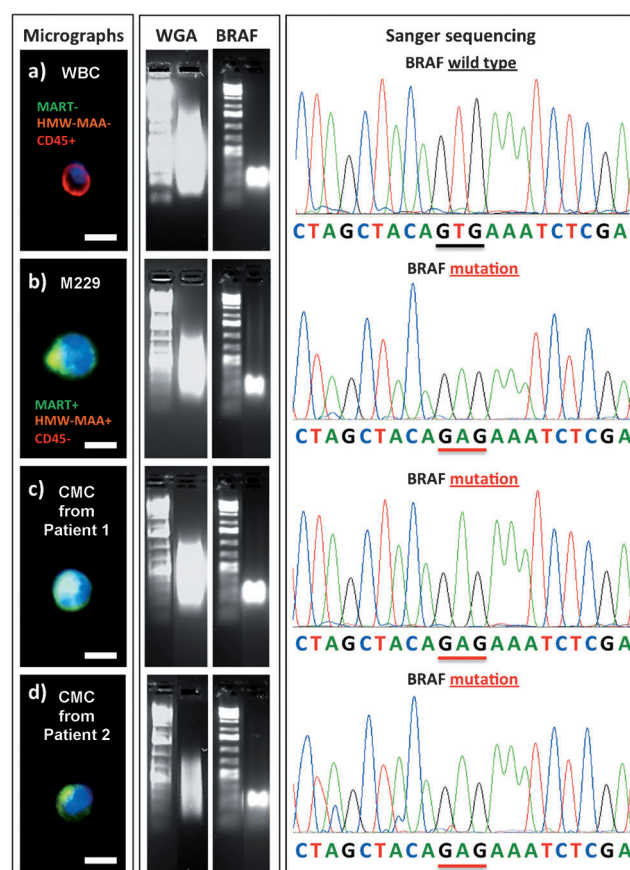


Figure 4. Left: Fluorescent micrographs of a) a negative control WBC, b) an M229 melanoma cell isolated from control blood sample, and c, d) two CMCs isolated from patients. Scale bar = 15 μm. Middle: Results from WGA and PCR amplification using a BRAF-specific primer. Right: Sanger sequencing of the individually isolated cells.

ing for a key melanoma drug target, the $BRAF^{V600E}$ mutation. Most importantly, the $BRAF^{V600E}$ mutation detected in single CMCs matched that detected in the tumor biopsies of the patients, supporting a positive correlation between CMCs and their tumor origin.

Received: October 20, 2012

Revised: December 20, 2012

Published online: February 21, 2013

Keywords: cancer · cancer diagnosis · circulating tumor cells · melanoma · single-cell analysis

- [1] a) R. Bernards, R. A. Weinberg, *Nature* **2002**, *418*, 823; b) K. Pantel, R. H. Brakenhoff, *Nat. Rev. Cancer* **2004**, *4*, 448–456; c) K. Pantel, C. Alix-Panabieres, *Trends Mol. Med.* **2010**, *16*, 398–406; d) J. Kaiser, *Science* **2010**, *327*, 1072–1074; e) C. Criscitiello, C. Sotiriou, M. Ignatiadis, *Curr. Opin. Oncol.* **2010**, *22*, 552–558.
- [2] a) M. Cristofanilli, et al., *N. Engl. J. Med.* **2004**, *351*, 781–791; b) S. Riethdorf, et al., *Clin. Cancer Res.* **2007**, *13*, 920–928; c) D. R. Shaffer, et al., *Clin. Cancer Res.* **2007**, *13*, 2023–2029; d) S. Nagrath, et al., *Nature* **2007**, *450*, 1235–1239.
- [3] a) G. Vona, et al., *Am. J. Pathol.* **2000**, *156*, 57–63; b) S. Zheng, H. Lin, J. Q. Liu, M. Balic, R. Datar, R. J. Cote, Y. C. Tai, *J. Chromatogr. A* **2007**, *1162*, 154–161; c) A. A. Adams, et al., *J. Am. Chem. Soc.* **2008**, *130*, 8633–8641; d) S. J. Tan, L. Yobas, G. Y. Lee, C. N. Ong, C. T. Lim, *Biomed. Microdevices* **2009**, *11*, 883–892; e) S. L. Stott, et al., *Proc. Natl. Acad. Sci. USA* **2010**, *107*, 18392–18397; f) J. P. Gleghorn, E. D. Pratt, D. Denning, H. Liu, N. H. Bander, S. T. Tagawa, D. M. Nanus, P. A. Giannakakou, B. J. Kirby, *Lab Chip* **2010**, *10*, 27–29; g) S. J. Tan, R. L. Lakshmi, P. Chen, W. T. Lim, L. Yobas, C. T. Lim, *Biosens. Bioelectron.* **2010**, *26*, 1701–1705; h) U. Dharmasiri, S. K. Njoroge, M. A. Witek, M. G. Adebiyi, J. W. Kamande, M. L. Hupert, F. Barany, S. A. Soper, *Anal. Chem.* **2011**, *83*, 2301–2309; i) M. N. Dickson, P. Tsinberg, Z. L. Tang, F. Z. Bischoff, T. Wilson, E. F. Leonard, *Biomicrofluidics* **2011**, *5*, 1–15; j) A. Lecharpentier, P. Vielh, P. Perez-Moreno, D. Planchard, J. C. Soria, F. Farace, *Br. J. Cancer* **2011**, *105*, 1338–1341; k) K. Pantel, R. H. Brakenhoff, B. Brandt, *Nat. Rev. Cancer* **2008**, *8*, 329–340; l) S. Riethdorf, K. Pantel, *Ann. N. Y. Acad. Sci.* **2010**, *1210*, 66–77.
- [4] a) S. Wang, et al., *Angew. Chem.* **2011**, *123*, 3140–3144; *Angew. Chem. Int. Ed.* **2011**, *50*, 3084–3088; b) S. Hou, et al., *Adv. Mater.* DOI: 10.1002/adma.201203185; c) Q. Shen, et al., *Adv. Mater.* DOI: 10.1002/adma.201300082.
- [5] S. Wang, et al., *Angew. Chem.* **2009**, *121*, 9132–9135; *Angew. Chem. Int. Ed.* **2009**, *48*, 8970–8973.
- [6] J. Sekine, S. C. Luo, S. Wang, B. Zhu, H.-R. Tseng, H. H. Yu, *Adv. Mater.* **2011**, *23*, 4788–4792.
- [7] N. Zhang, et al., *Adv. Mater.* **2012**, *24*, 2756–2760.
- [8] a) K. E. Fischer, et al., *Nano Lett.* **2009**, *9*, 716–720; b) A. S. G. Curtis, M. Varde, *J. Natl. Cancer Inst.* **1964**, *33*, 15–26; c) W. F. Liu, C. S. Chen, *Adv. Drug Delivery Rev.* **2007**, *59*, 1319–1328.
- [9] A. D. Stroock, S. K. Dertinger, A. Ajdari, I. Mezic, H. A. Stone, G. M. Whitesides, *Science* **2002**, *295*, 647–651.
- [10] A. A. Powell, et al., *PLoS One* **2012**, *7*, e33788.
- [11] X. Xu, et al., *Cell* **2012**, *148*, 886–895.
- [12] a) H. J. Shin, C. H. Lee, I. H. Cho, Y. J. Kim, Y. J. Lee, I. A. Kim, K. D. Park, N. Yui, J. W. Shin, *J. Biomater. Sci. Polym. Ed.* **2006**, *17*, 103–119; b) X. Xin, M. Hussain, J. J. Mao, *Biomaterials* **2007**, *28*, 316–325; c) S. J. Kim, D. H. Jang, W. H. Park, B. M. Min, *Polymer* **2010**, *51*, 1320–1327.
- [13] Anti-CD146 is a melanoma-specific antibody used in the CellSearch circulating melanoma cell assay. See its clinical studies in: C. Rao, T. Bui, M. Connelly, G. Doyle, I. Karydis, M. R. Middleton, G. Clack, M. Malone, F. A. Coumans, L. W. Terstappen, *Int. J. Oncol.* **2011**, *38*, 755–760.
- [14] J. Sun, et al., *Cancer Res.* **2010**, *70*, 6128–6138.
- [15] a) G. Bollag, et al., *Nature* **2010**, *467*, 596–599; b) J. A. Sosman, et al., *N. Engl. J. Med.* **2012**, *366*, 707–714; c) P. B. Chapman, et al., *N. Engl. J. Med.* **2011**, *364*, 2507–2516; d) K. T. Flaherty, et al., *N. Engl. J. Med.* **2010**, *363*, 809–819.
- [16] a) J. N. S ndergaard, et al., *J. Transl. Med.* **2010**, *8*, 39; b) R. Nazarian, et al., *Nature* **2010**, *468*, 973–977.
- [17] a) H. Shi, X. Kong, A. Ribas, R. S. Lo, *Cancer Res.* **2011**, *71*, 5067–5074; b) P. I. Poulidakos, et al., *Nature* **2011**, *480*, 387–390.